G. Salvadori, *J. Chem. Soc.*, B, 769 (1966).
21. J. W. Moore and R. G. Pearson, *Kinetics and Mechanism*, John Wiley & Sons, New York, 130 (1980).
22. J. C. Martin and T. M. Barthazor, *J. Am. Chem. Soc.*, **99**, 152 (1977); C. W. Tullock, D. D. Caffman, and E. L. Muetterties, *J. Am. Chem. Soc.*, **86**, 357 (1964); K. O. Christe, E. C. Curtis, C. J. Schock, and D. Pilipovich, *Inorg. Chem.*, **11**, 1679 (1972).
23. R. D. Gilliom, *Introduction to Physical Organic Chemistry*, Addison-Wesley Pub. Co., London, 151 (1970).
24. W. P. Jencks and J. Carriuolo, *J. Am. Chem. Soc.*, **83**, 1743 (1961).
25. L. H. Funderburk, L. Aldwin, and W. P. Jencks, *J. Am. Chem. Soc.*, **100**, 5444 (1978).
26. J. M. Harris, A. Becker, J. F. Fagan, and F. A. Walden, *J. Am. Chem. Soc.*, **96**, 4484 (1974); J. M. Harris, D. C. Clark, A. Becker, and J. F. Fagan, *J. Am. Chem. Soc.*, **96**, 4478 (1974).
27. J. Kaspi and Z. Rappoport, *Tetrahedron Lett.*, 2035 (1977).
28. T. Ando and S.-ichi Tsukamoto, *Tetrahedron Letter.*, 2775 (1977).
29. D. A. Da Roza, L. J. Andrews, and R. M. Keefer, *J. Am. Chem. Soc.*, **95**, 7003 (1973); V. J. Shiner, Jr., W. Dowd, R. D. Fisher, S. R. Hartshorn, M. A. Kessick, L. Milakofsky, and M. W. Rapp, *ibid.*, **91**, 4838 (1969).
30. J. A. Riddick, W. B. Bunger, and T. K. Sakano, *Organic Solvents; Physical Properties and Methods of Purification*, MeOH(D)=32.6, $MeNO_2$(D)=38.6, $PhNO_2$(D)=34.6, EG (D)=37.7 at 25℃, respectively.
31. V. Gold and D. Bethell, *Adv. Phys. Org. Chem.*, **14**, 32, Academic Press, London (1977); A. H. Fainberg and S. Winstein, *J. Am. Chem. Soc.*, **78**, 2770 (1956); T. W. Bentley, F. L. Schadt, and P. v. R. Schleyer, *J. Am. Chem. Soc.*, **95**, 992 (1972).

Preparation and Characterization of Chromium Oxide Supported on Zirconia

Jong Rack Sohn*, Sam Gon Ryu, Man Young Park, and Young Il Pae†

Department of Industrial Chemistry, Kyungpook National University, Taegu 702-701
†Department of Chemistry, National Science College Ulsan University, Ulsan 680-749
Received March 31, 1992

Chromium oxide/zirconia catalysts were prepared by dry impregnation of powdered $Zr(OH)_4$ with $(NH_4)_2CrO_4$ aqueous solution. The characterization of prepared catalysts was performed using FTIR, XPS, XRD and DTA methods, and by the measurement of surface area. The addition of chromium oxide to zirconia shifted the transitions of ZrO_2 from amorphous to tetragonal phase and from tetragonal to monoclinic phase to higher temperature due to the strong interaction between chromium oxide and zirconia, and the specific surface area of catalysts increased in proportion to the chromium oxide content. Since the ZrO_2 stabilizes supported chromium oxide, chromium oxide was well dispersed on the surface of zirconia, and α-Cr_2O_3 was observed only at the calcination temperature above 1173 K. Upon the addition of only small amount of chromium oxide (1 wt% Cr) to ZrO_2, both the acidity and acid strength of catalyst increased remarkably, showing the presence of two kinds of acid sites on the surface of CrO_x/ZrO_2-Brönsted and Lewis.

Introduction

Supported chromium oxide catalysts are being used for the polymerization, hydrogenation, dehydrogenation, oxidation-reduction reactions between environmentally important molecules such as CO and NO.[1-5] Recently, many efforts have involved the characterization of these catalysts in an attempt to find the appropriate reaction mechanisms. The titrations to determine the oxidation state of the chromium used in conjunction with infrared and electron paramagnetic resonance spectroscopies have provided much information dealing with these questions. So far, however, they have been studied mainly on silica and alumina,[6-8] and only a little work was studied for the ZrO_2 support.[9,10]

Zirconia is an important material due to its interesting thermal and machanical properties and so has been investigated as a support and catalysts in recent years. Different papers have been devoted to the studies of ZrO_2 catalytic activity in the important reactions such as methanol and hydrocarbon syntheses from CO and H_2, from CO_2 and H_2[11,12], or from alcohol dehydration.[13,14] Zirconia has been extensively used as a support for metals or incorporated in supports to stabilize them or to make them more resistant to sintering.[15-17] ZrO_2 activity and selectivity highly depend on the methods of preparation and treatment used. In particular, in the previous papers from this laboratory, it has been shown that NiO-ZrO_2 and ZrO_2 modified with sulphate ion are very active for acid-catalyzed reactions, even at room temperature.[18-20] The high catalytic activities in the above reactions were attributed to the enhanced acidic properties

of the modified catalysts, which originate from the inductive effect of S=O bonds of the complex formed by the interaction of oxides with the sulphate ion.

It is well known that the dispersion, the oxidation state, and the structural features of supported species may strongly depend on the support. Structure and physicochemical properties of supported metal oxides are considered to be different compared with bulk metal oxides because of their interaction with supports. This paper describes the preparation and characterization of chromium oxide supported on zirconia.

The characterization of the samples was performed by means of FTIR, XRD, XPS and DTA, and by the measurement of surface area.

Experimental

Catalyst Preparation. The precipitate of $Zr(OH)_4$ was obtained by adding aqueous ammonia slowly into an aqueous solution of zirconium oxychloride at room temperature with stirring until the pH of mother liquor reached about 8. The precipitate thus obtained was washed thoroughly with distilled water until chloride ion was not detected, and was dried at room temperature for 12 h. The dried precipitate was powdered below 100 mesh.

The catalysts containing various chromium contents were prepared by dry impregnation of powdered $Zr(OH)_4$ with $(NH_4)_2CrO_4$ aqueous solution followed by calcining at different temperatures for 1.5 h air. This series of catalysts are denoted by their weight percentage of chromium. For example, 1-CrO_x/ZrO_2 indicates the catalyst containing 1 weight % chromium.

Physicochemical Characterization. FTIR spectra were obtained in a gas cell at room temperature using Mattson Model GL 6030 E spectrophotometer. The self-supporting catalyst was pressed into wafers weighing 9 mg/cm^2. Prior to recording the spectra the sample was heated under vacuum at 673-773 K for 1.5 h.

Catalysts were checked in order to determine the structure of the support as well as that of chromium oxide by means of a Jeol Model JDX-8030 diffractometer, employing Cu Kα (Ni-filtered) radiation.

X-ray photoelectron spectra were obtained with a VG Scientific Model ESCALAB MK-11 spectrometer. Al Kα and Mg Kα were used as the excitation source, usually at 12 kV, 20 mA. The analysis chamber was at 10^{-9} torr or better and the spectra of samples, as fine powder, were analyzed. However, to examine the redox-behaviour of catalysts, some samples were pressed onto a plate, treated with H_2 and O_2 in a separate gas cell, and transferred into a analysis chamber without exposure to air.

Binding energies were referenced to the C_{1s} level at 285.0 eV.

DTA measurements were performed in flowing Ar (30 ml/min) using a differential thermal analyzer (Dupon 2100). The heating rate was 5-10 K/min. For each experiment 30-50 mg of sample was used.

The specific surface area was determined by the BET method through the N_2 adsorption at 77 K. Chemisorption of ammonia was also employed as a measure of the acidity of catalysts. The amount of chemisorption was determined based on the irreversible adsorption of ammonia.[21]

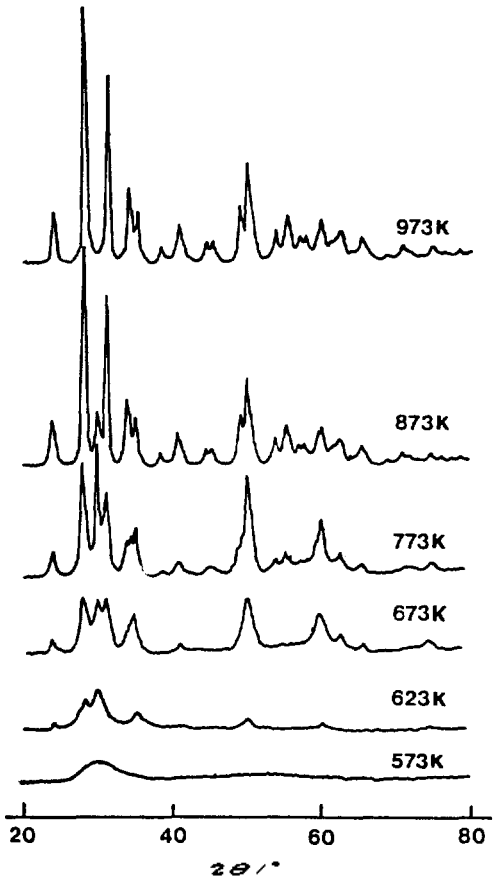

Figure 1. X-ray diffraction patterns of ZrO_2 calcined at different emperatures for 1.5 h.

Results and Discussion

X-ray Diffraction. The crystalline structures of catalysts calcined in air at different temperatures for 1.5 h were examined. Figure 1 represents X-ray diffraction patterns of ZrO_2 calcined in air at different temperatures. Based on our patterns ZrO_2 was amorphous up to 573 K, a mixture of tetragonal and monoclinic forms at rising temperatures of 623-873 K, and a monoclinic phase at 973 K. Three crystal modifications of the tetragonal, monoclinic and cubic have been reported.[22,23]

In the cases of supported catalysts, the crystalline structures of samples are different from that of ZrO_2. For the 5-CrO_x/ZrO_2, as shown in Figure 2, ZrO_2 is amorphous up to 723 K. In other words, the transition temperature from the amorphous to tetragonal phase is higher by 150 K than that of pure ZrO_2. X-ray diffraction data indicated the tetragonal phase of ZrO_2 at 773 K, a mixture of the tetragonal and monoclinic ZrO_2 at 873-1073 K, and a mixture of the tetragonal and monoclinic ZrO_2, and α-Cr_2O_3 at 1173 K. It is assumed that the strong interaction between chromium oxide and ZrO_2 prohibits the transition of ZrO_2 from amorphous to tetragonal. The presence of chromium seems to influence strongly the development of textural properties of ZrO_2 depending on the temperature. Moreover, for the sample of 10-CrO_x/ZrO_2 the transition temperature from the

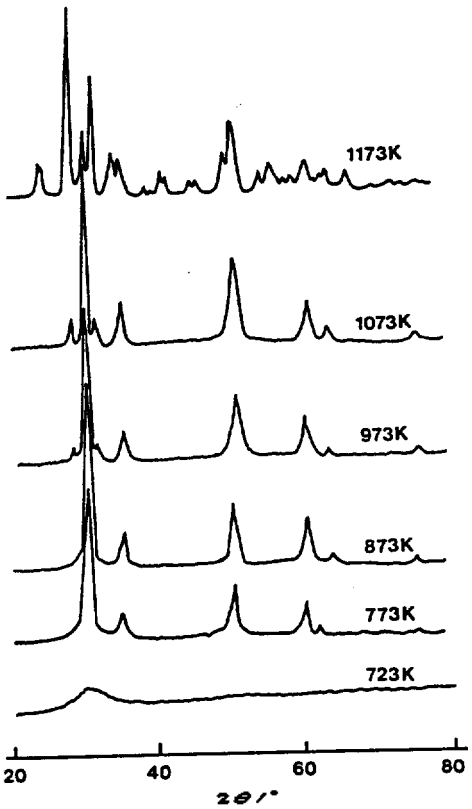

Figure 2. X-ray diffraction patterns of 5-CrO_x/ZrO_2 calcined at different temperatures for 1.5 h.

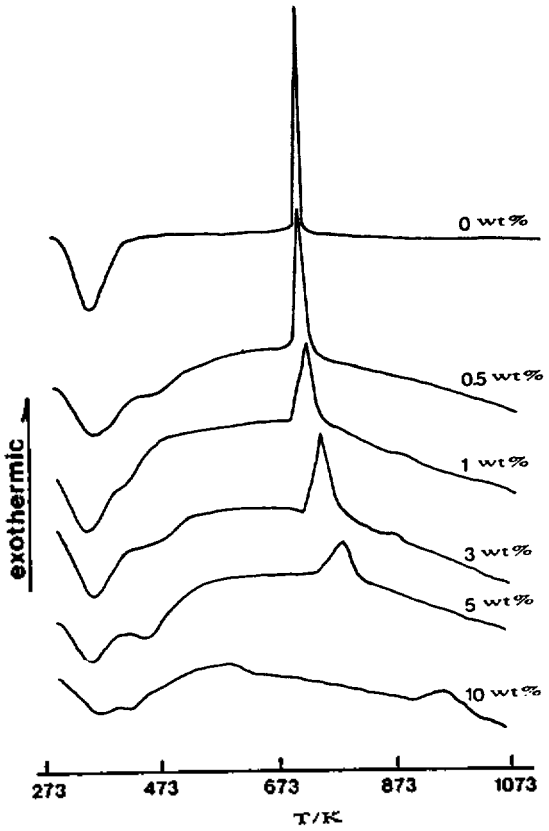

Figure 4. DTA curves of precursors of catalysts, $Zr(OH)_4$ and $(NH_4)_2CrO_4/Zr(OH)_4$.

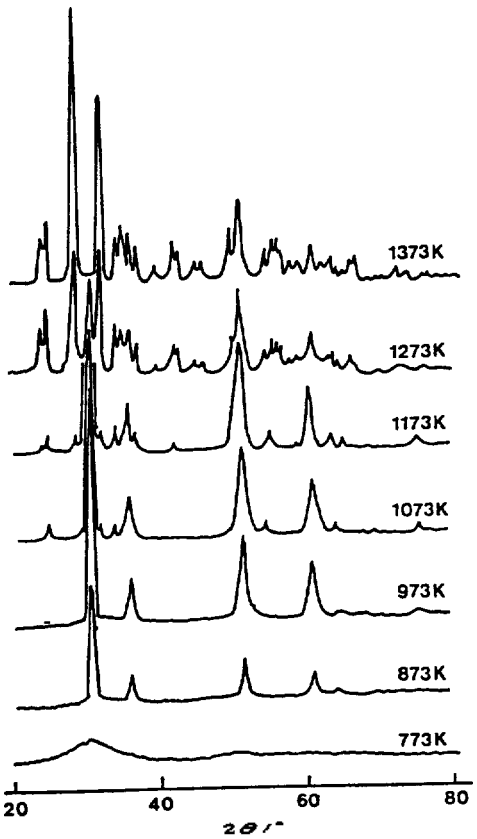

Figure 3. X-ray diffraction patterns of 10-CrO_x/ZrO_2 calcined at different temperatures for 1.5 h.

amorphous to tetragonal phase is higher by 200 K than that of pure ZrO_2 as can be seen in Figure 3. That is, the more is the chromium content, the higher is the transition temperature. These results are in good agreement with DTA data which will be discussed in the next. 10-CrO_x/ZrO_2 is amorphous up to 773 K, tetragonal at 873-973 K, a mixture of the tetragonal and monoclinic ZrO_2 at 1073 K, a mixture of the tetragonal and monoclinic ZrO_2, and α-Cr_2O_3 at 1173-1273 K, and a mixture of the monoclinic ZrO_2 and α-Cr_2O_3 at 1373 K. Any phase of chromium oxide is not observed at calcination temperature up to 1073 K, indicating a good dispersion of chromium oxide on the surface of ZrO_2 support due to the strong interaction between them. As shown in Figures 2 and 3, α-Cr_2O_3 phase is observed only in the samples calcined at above 1173 K, showing that the ZrO_2 support stabilizes supported chromium oxide, and chromium oxide is well dispersed on the surface of ZrO_2 under the calcination temperature below 1173 K.

It is also of interest to examine the influence of chromium oxide on the transition temperature of ZrO_2 from the tetragonal to monoclinic. Comparisons of Figures 1-3 show that the stabilization of the tetragonal ZrO_2 is observed on CrO_x/ZrO_2 samples. In view of X-ray diffraction patterns, the calcination temperatures at which monoclinic phase is observed initially are 623 K for pure ZrO_2, 673 K for 1-CrO_x/ZrO_2, 873 K for 5-CrO_x/ZrO_2, and 973 K for 10-CrO_x/ZrO_2. That is, the transition temperature increases with increasing chromium oxide content. This can be also explained by the delay of transition from the tetragonal to monoclinic due to the

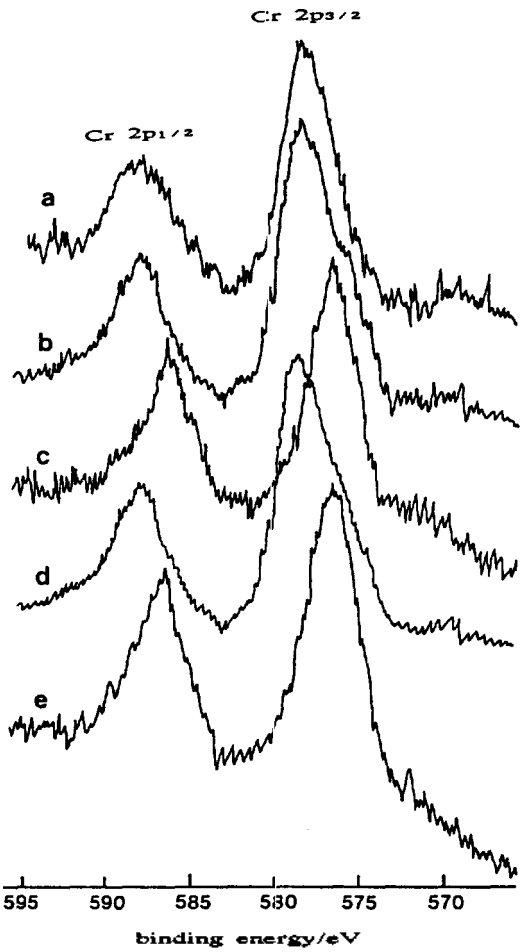

Figure 5. Cr 2*p* XPS of 3-CrO_x/ZrO_2 treated under various conditions: (a) uncalcined sample; (b) sample calcined at 873 K; (c) after reduction of (b) sample with H_2 at 823 K; (d) after reoxidation of (c) sample with O_2 at 823 K; (e) after reaction of (b) sample with *n*-hexane at 823 K.

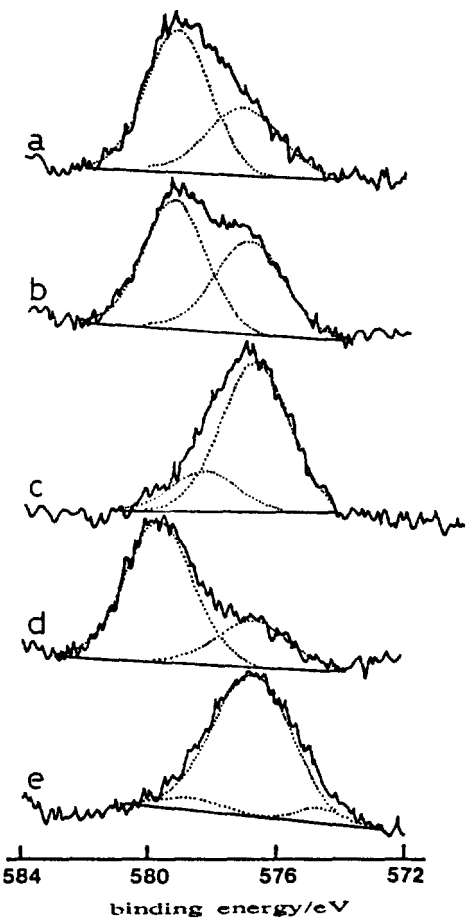

Figure 6. Cr $2p_{3/2}$ fitted for XPS of 3-CrO_x/ZrO_2 treated under various conditions: (a) uncalcined sample; (b) sample calcined at 873 K; (c) after reduction of (b) sample with H_2 at 823 K; (d) after reoxidation of (c) sample with O_2 at 823 K; (e) after reaction of (b) sample with *n*-hexane at 823 K.

strong interaction between chromium oxide and zirconia, in analogy with the delay of transition from the amorphous to tetragonal, as was described in the above.

Thermal Analysis. Based on the X-ray diffraction patterns, the structures of catalysts are different from each other depending on the calcination temperature. To examine the thermal properties of precursors of catalysts more clearly, their thermal analyses were carried out. The result are shown in Figure 4. For pure ZrO_2, the DTA curve shows an endothermic peak in the temperature range 303-453 K due to water elimination, and a sharp exothermic peak at 703-743 K due to the ZrO_2 crystallization. In the case of CrO_x/ZrO_2 catalysts, an additional endothermic peak appears at about 473 K due to the evolution of NH_3 produced from $(NH_4)_2CrO_4$. Interestingly, chromium oxide influences the phase transition of ZrO_2 from the amorphous to tetragonal. As Figure 4 shows, the exothermic peak due to the phase transition appears at about 723 K for pure ZrO_2, while for CrO_x/ZrO_2 samples it is shifted to higher temperatures. The degree of shift increases and the shape of peak becomes broad with increasing chromium content. Consequently, the exothermic peak appears at 923-973 K for 10-CrO_x/ZrO_2. These results are in good agreement with those of X-ray resurts described above. It is relevant that the strong interaction between chromium oxide and zirconia delays the transition of ZrO_2 from the amorphous to tetragonal. A similar result has been observed by Sohn *et al.*[20,24] for silica and sulfate ion additions.

X-ray Photoelectron Spectra. The difficulty in the study of supported chromium oxide comes from the simultaneous presence of different oxidation states. Figure 5 shows the Cr 2*p* spectra of 3-CrO_x/ZrO_2 treated under various conditions. The shape of peaks and binding energies of 2*p* electron are different depending on the treatment conditions, indicating that the oxidation state of chromium varies with the treatment process.

To obtain further information on the oxidation state, the spectrum in the Cr $2p_{3/2}$ region was analyzed by appropriate curve fitting and the presence of two or three components was confirmed, as shown in Figure 6. For the noncalcined and calcined samples, we have obtained a Cr $2p_{3/2}$ binding energy of 579.3 eV due to Cr(VI) and a binding energy of 576.7 eV identified as Cr(III). Cimino and coworkers[25] have measured Cr 2*p* binding energies for a variety of different chromium compounds. The corresponding Cr $2p_{3/2}$ binding

Table 1. Percentage of Chromium Species from The Area of The Fitted Bands in The Cr $2p_{3/2}$ XPS Region

Treatment conditions \ Cr species	Cr^{6+}	Cr^{3+}	Cr^{0}
Uncalcined sample	65	35	
Calcined in air at 873 K	54	46	
After reduction with H_2 at 823 K	19	81	
After oxidation with O_2 at 823 K	59	41	
After reaction with *n*-hexane at 823 K	3	89	7

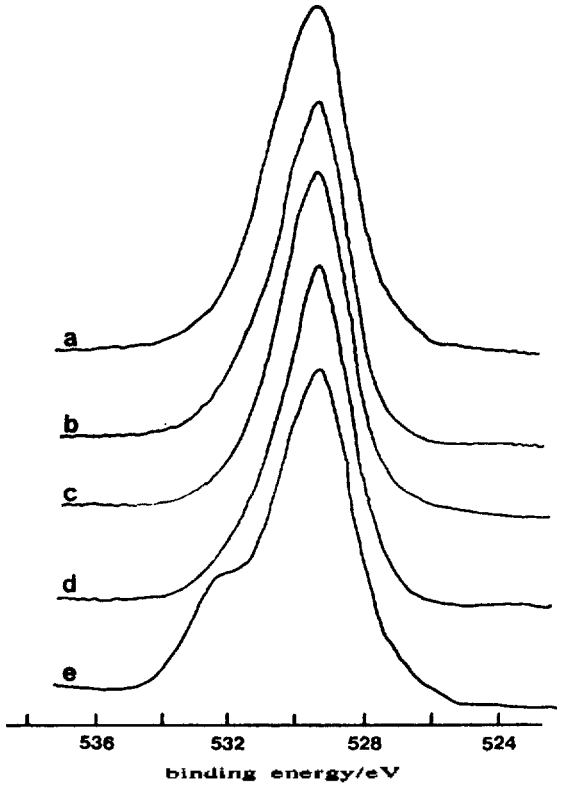

Figure 7. O_{1s} XPS of 3-CrO_x/ZrO_2 treated under various conditions: (a) uncalcined sample; (b) sample calcined at 873 K; (c) after reduction of (b) sample with H_2 at 823 K; (d) after reoxidation of (c) sample with O_2 at 823 K; (e) after reaction of (b) sample with *n*-hexane at 823 K.

energies for CrO_3 and Cr_2O_3 are 579.9 and 576.8 eV, respectively.

The result of quantitative analysis for the chromium oxidation state are listed in Table 1. It is noted that the amount of Cr(III) increases to some extent by the calcination at 873 K. However, Cr(VI) concentration of the sample calcined at 873 K is quite large, being 54% of the total Cr concentration, indicating that the ZrO_2 support stabilizes supported chromium oxide as follows:

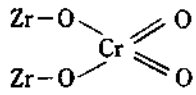

However, when the sample b in Figure 6 was treated with H_2 at 873 K for 6 min, Cr(VI) species was easily reduced to Cr(III) species, as illustrated in Figure 6(c) and Table 1. The sample c was reoxidized with O_2 at 823 K for 6 min and its XPS result is shown in Figure 6(d). The Cr(VI)/Cr (III) ratio increased, which indicates that redox process is reversible. 1 μl of *n*-hexane was reacted successively 10 times over the sample calcined at 873 K at reaction temperature of 823 K. XPS of catalyst after reaction is illustrated in Figure 6(e), resulting in the increase of Cr(III) concentration. In this case we have also obtained a Cr $2p_{3/2}$ binding energy of 574.7 eV assigned to chromium metal.[26] This again suggests reduction from Cr(VI) to Cr(III) or Cr(0) by *n*-hexane.

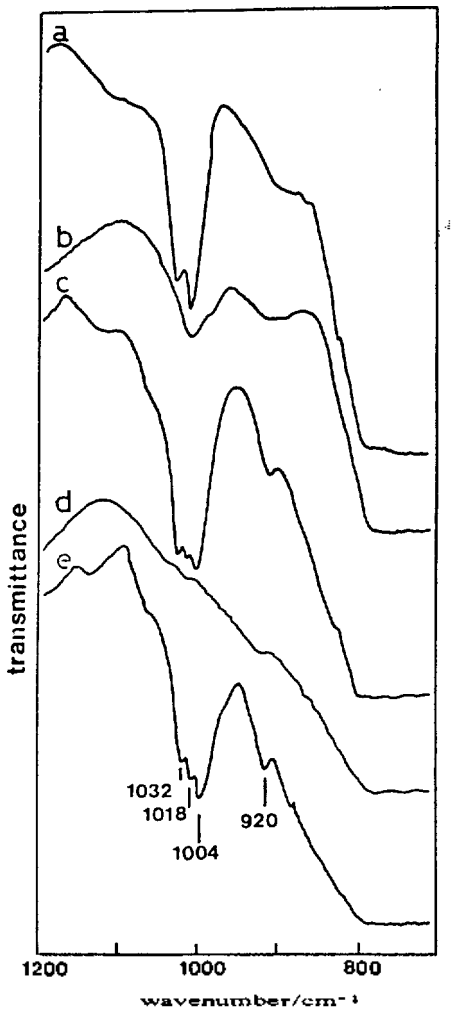

Figure 8. IR spectra of 1-CrO_x/ZrO_2 treated under various conditions: (a) after evacuation at 773 K for 1 h; (b) after evacuation at 773 K for 2 h; (c) after oxidation of (b) sample with O_2 (50 torr) at 773 K for 1 h; (d) after reduction of (c) sample with CO (50 torr) at 773 K for 0.5 h; (d) after reoxidation of (d) sample with O_2 (50 torr) at 773 K for 0.5 h.

Figure 7 shows O_{1s} spectra of 3-CrO_x/ZrO_2 treated under various conditions. In all the spectra the O_{1s} peak at lower binding energy, 529.2 eV corresponds to lattice oxide ions.[27] However, for the sample reacted with *n*-hexane, the O_{1s} peak appeared at higher binding energy, 532 eV. This peak can be attributed to a carbonate species formed during the catalytic reaction of *n*-hexane. Recently, Gonzalez *et al.*[27] have characterized the surface state of some metal oxides by XPS.

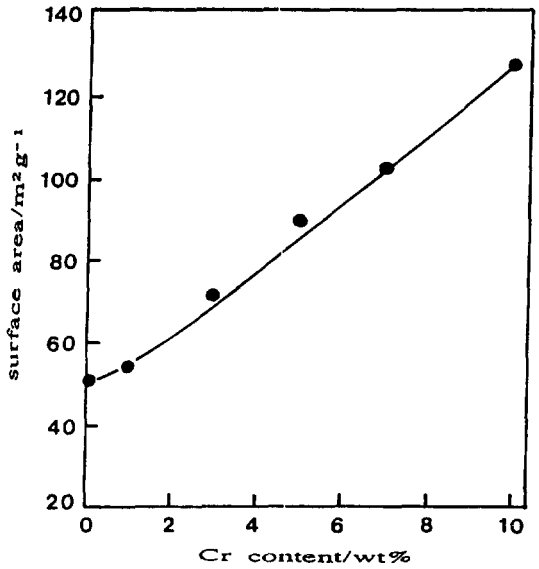

Figure 9. Variation of surface area of CrO_x/ZrO_2 calcined at 873 K with chromium content.

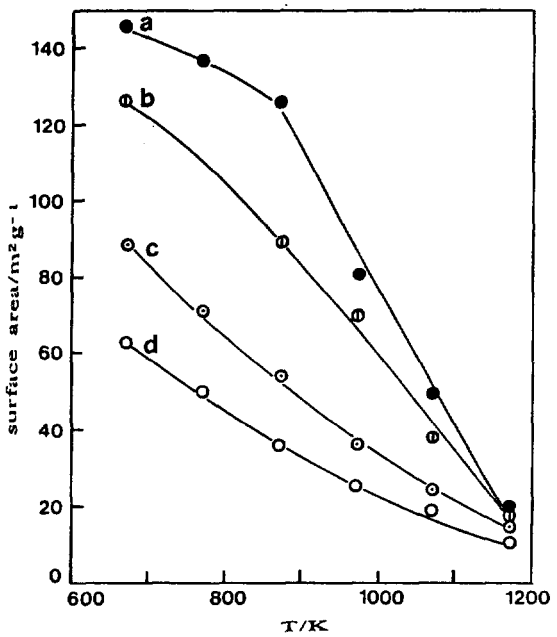

Figure 10. Variations of surface area for ZrO_2 and some CrO_x/ZrO_2 samples against calcination temperature: (a) 10-CrO_x/ZrO_2; (b) 5-CrO_x/ZrO_2; (c) 1-CrO_x/ZrO_2; (d) ZrO_2.

They reported that the second O_{1s} peak appearing at the high binding energy side of the main peak corresponding to the oxide anions has been attributed to carbonate species.

IR Spectra. Figure 8 shows the IR spectra of 1-CrO_x/ZrO_2 treated under various conditions. After evacuation at 773 K for 1 h, three bands at 1032, 1018 and 920 cm^{-1} were observed. The doublet at 1032 and 1018 cm^{-1} is assigned to the asymmetric and symmetric stretching modes, respectively, of surface chromates.[9] The broad band at around 900 cm^{-1} is typical of chromium-oxygen groups of a lower double-bond character. However, upon evacuation at 773 K for 2 h, the intensities of doublet bands decrease remarkably due to the removal of surface oxygen. Reoxidation of the sample b in Figure 8 was performed by the addition of O_2 (50 torr) at 773 K for 0.5 h and then IR spectrum was recorded at room temperature [Figure 8(c)]. Heating in oxygen at 773 K nearly restored the situation observed in Figure 8(a) and an additional band at 1004 cm^{-1} assigned to Cr=O species is observed. The weak and sharp band at 920 cm^{-1} can be interpreted as due to the blue shift of the Zr-O-Cr mode caused by Cr oxidation. Upon reduction of oxidized sample c in Figure 8 with CO at 773 K, the intensities of all bands in the 1100-900 cm^{-1} region decrease as shown in Figure 8(d). Upon introduction of O_2 (50 torr) to the sample reduced with CO and heating at 773 K for 0.5 h, the bands at 1032, 1018, 1004 and 920 cm^{-1} are also recovered. Complete reversibility is observed after redox process in good agreement with XPS results.

Surface Properties of CrO_x/ZrO_2 Catalyst. It is necessary to examine the effect of chromium oxide on the surface properties of catalysts, such as, sepecific surface area, acidity, and acid strength. The specific surface areas of samples calcined at 873 K for 1.5 h are plotted as a function of chromium content in Figure 9. The presence of chromium oxide strongly influences the surface area in comparison with the pure ZrO_2. Specific surface areas of CrO_x/ZrO_2 are much larger than that of pure ZrO_2 calcined at the same temperature, showing that surface area increases gradually with increasing chromium content. In fact, a good reproducibility for the increase of surface area with chromium content appeared. It seems like that the strong interaction between chromium oxide and ZrO_2 protects catalysts from sintering. The dependence of antisintering effect on chromium oxide content is clear from Figure 9. These results are correlated with the fact that the transition temperature of ZrO_2 from the amorphous to tetragonal increases with increasing chromium oxide content in DTA experiment. These results are also in agreement with those of phase transition of ZrO_2 observed in X-ray diffraction patterns as illustrated in Figure 1-3.

In addition to chromium oxide content, calcination temperature influences the surface area. When pure ZrO_2 and some CrO_x/ZrO_2 samples are subjected to calcining in air at a given temperature, the results obtained are plotted in Figure 10 as a function of calcination temperature. The antisintering effect of chromium oxide is greater at lower calcination temperature than at higher temperature. As illustrated in Figure 10, the difference of surface area between pure ZrO_2 and CrO_x/ZrO_2 calcined at 1173 K is very small compared with the cases of samples calcined at lower temperatures. For the CrO_x/ZrO_2 samples, α-Cr_2O_3 crystalline was observed at the calcination temperature above 1173 K as described in the results of X-ray diffraction. Therefore, it seems like that the small antisintering effect of chromium oxide at the calcination temperature of 1173 K is related to the formation of α-Cr_2O_3 and consequently the weak interaction between α-Cr_2O_3 and zirconia.

The acid strength of the catalysts was examined by a color change method, using Hammett indicator[28] in dried benzene. Since it was very difficult to observe the color of indicators adsorbed on catalysts of high chromium oxide content, a low percentage of chromium content (0.1 wt%) was used in this experiment. The results are listed in Table 2. In this

Table 2. Acid Strength of 0.1-CrO_x/ZrO_2 and ZrO_2

Hammett indicator	pK_a value of indicator	CrO_x/ZrO_2*	CrO_x/ZrO_2**	CrO_x/ZrO_x***	ZrO_2
Dicinnamalacetone	−3.0	+	+	+	+
Benzalacetophenone	−5.6	+	+	+	+
Anthraquinone	−8.2	+	+	+	−
Nitrobenzene	−12.4	+	+	−	−
2,4-Dinitrofluorobenzene	−14.5	+	+	−	−

*Calcined in air at 873 K; **Oxidized with O_2 at 773 K; ***Reduced with CO at 773 K.

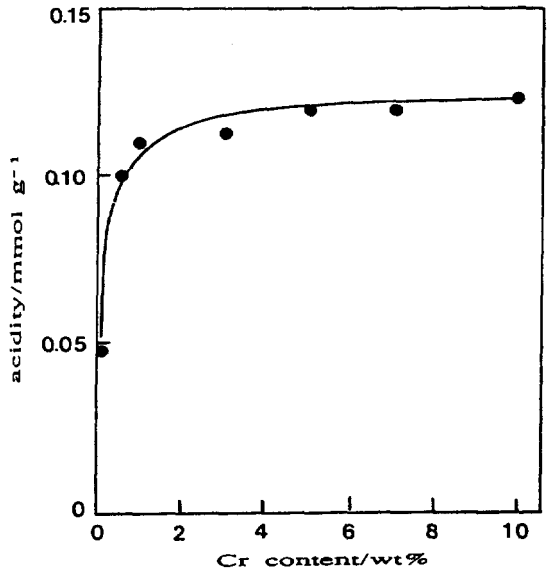

Figure 11. Acidity of CrO_x/ZrO_2 against chromium content.

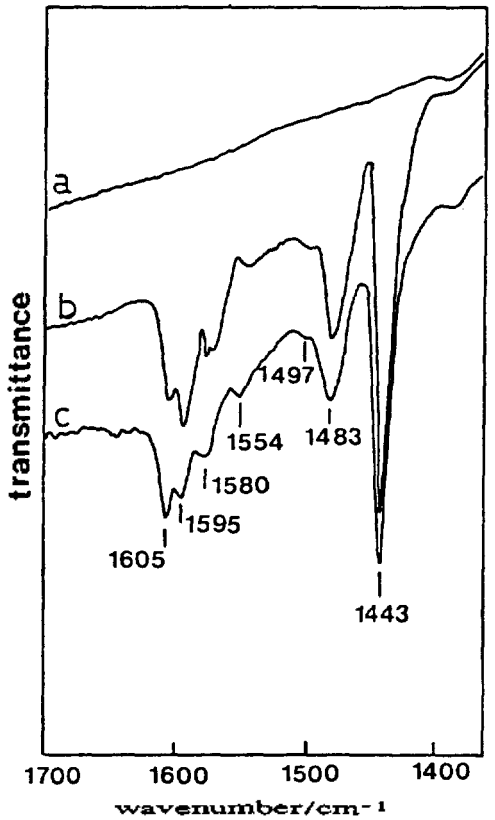

Figure 12. IR Spectra of pyridine adsorbed on 1-CrO_x/ZrO_2: (a) background of 1-CrO_x/ZrO_2 after evacuation at 773 K for 1 h; (b) pyridine adsorbed on (a) sample followed by evacuating at room temperature for 1 h; (c) pyridine adsorbed on (a) sample followed by evacuating at 523 K for 1 h.

table, (+) indicates that the color of the base form is changed to that of the conjugated acid form. ZrO_2 evacuated at 673 K for 1 h has an acid strength $H_o \leq -5.6$, while 0.1-CrO_x/ZrO_2 is estimated to have a $H_o \leq -14.5$, indicating the formation of new acid sites stronger than those of single oxide components. The acid strength of 0.1-CrO_x/ZrO_2 oxidized with O_2 at 773 K is also found to be $H_o \leq -14.5$. However, the acid strength of 0.1-CrO_x/ZrO_2 reduced with CO at 773 K for 0.5 h was found to be $H \leq -8.2$. Acids stronger than $H_o \leq -11.93$, which corresponds to the acid strength of 100% H_2SO_4, are superacids.[29] Consequently, CrO_x/ZrO_2 catalysts would be solid superacids. The superacidic property is attributed to the double bond nature of the Cr=O in the complex formed by the interaction of ZrO_2 with chromate, in analogy with the case of ZrO_2 modified with sulphate ion.[18-20]

The acidity of catalysts, as determined by the amount of NH_3 irreversibly adsorbed at 503 K[21], is plotted as a function of the chromium content in Figure 11. Although pure ZrO_2 shows the acidity of 0.05 meq/g, 1-CrO_x/ZrO_2 results in a remarkable increase in acidity (0.1 meq/g). As shown in Figure 11, the acidity increases abruptly upon the addition of 1 wt% chromium to ZrO_2, and then the acidity increases very gently with increasing chromium oxide content. Many combinations of two oxides have been reported to generate acid sites on the surface.[30-32] The combination of ZrO_2 and CrO_x generates stronger acid sites and more acidity as compared with the seperate components. A mechanism for the generation of acid sites by mixing two oxides has been proposed by Tanabe *et al.*.[30] They have suggested that the acidity generation is caused by excess of a negative or a positive charge in the model structure of a binary oxide related to the coordination number of a positive and a negative elements.

Infrared spectroscopic studies of pyridine adsorbed on solid surfaces have made it possible to distinguish Brönsted and Lewis acid sites.[33] Figure 12 shows the infrared spectra of pyridine adsorbed on 1-CrO_x/ZrO_2 evacuated at 773 K for 1 h. There are peaks at 1443, 1488, 1497, 1554, 1580, 1595 and 1605 cm^{-1} comprising the vibrational modes of pyridine after evacuation at room temperature. Many peaks are weakened after evacuation at 523 K. Consequently, this set of absorption peaks disappeared can be assigned to hydro-

gen-bonded pyridine.[34] The bands at 1554 and 1497 cm^{-1} are the characteristic peaks of pyridinium ion, which are formed on the Brönsted acid sites.[35] The other set of absorption peaks at 1443, 1482, 1580 and 1605 cm^{-1} is contributed by pyridine coordinatively bonded to Lewis acid sites. It is clear that both Brönsted and Lewis acid sites exist on the surface of CrO_x/ZrO_2 catalysts calcined at 873 K.

Conclusions

This paper has shown that a combination of FTIR, XPS, XRD and DTA can be used to perform the characterization of CrO_x/ZrO_2 catalysts prepared by dry impregnation. The strong interaction between chromium oxide and zirconia influences the physicochemical properties of prepared catalysts depending on the temperature. The presence of chromium oxide prohibits the transitions of zirconia from amorphous to tetragonal and from the tetragonal to monoclinic. The specific surface area of catalysts increases in proportion to the chromium oxide content. The Cr(VI) concentration in 1-CrO_x/ZrO_2 calcined at 873 K is very high, showing 54% of the total Cr concentration, but the α-Cr_2O_3 is observed only at the calcination temperature above 1173 K, indicating that the ZrO_2 support stabilizes supported chromium oxide, which is well dispersed on the surface of ZrO_2. By oxygen, hydrogen, carbon monoxide and *n*-hexane treatments, the redox behaviours from Cr(VI) to Cr(III) or vice versa are reversible. Upon the addition of only small amount of chromium oxide (1 wt% Cr) to ZrO_2, both the acidity and acid strength of catalyst increase remarkably, showing the presence of two kinds of acid sites on the surface of CrO_x/ZrO_2-Brönsted and Lewis.

Acknowledgement. This paper was supported by NON DIRECTED RESEARCH FUND, Korea Research Foundation, 1990.

References

1. J. P. Hogan, *J. Polymer Sci.*, **8**, 2637 (1970).
2. D. L. Myers and J. H. Lunsford, *J. Catal.*, **99**, 140 (1986).
3. A. Clark, *Catal. Rev.*, **3**, 145 (1969).
4. C. Groeneveld, P. P. M. M. Wittgen, A. M. van Kersbergen, P. L. M. Mestrom, C. E. Nuijten, and G. C. A. Schuit, *J. Catal.*, **59**, 153 (1979).
5. M. Shelef, K. Otto, and H. Gandhi, *J. Catal.*, **12**, 361 (1968).
6. M. P. McDaniel, *Adv. Catal.*, **33**, 47 (1985).
7. G. Ghiotti, E. Garrone, and A. Zecchina, *J. Mol. Catal.*, **46**, 61 (1988).
8. W. Hill and G. Öhlmann, *J. Catal.*, **123**, 147 (1990).
9. A. Cimino, D. Cordisch, S. Febbraro, D. Gazzoli, V. Indovina, M. Occhiuzzi, and M. Valigi, *J. Mol. Catal.*, **55**, 23 (1989).
10. T. Yamaguchi, M. Tan-No, and K. Tanabe, Preparation of Catalysts V, Elsevier, 567 (1991).
11. M. Y. He and J. G. Ekerdt, *J. Catal.*, **90**, 17 (1984).
12. T. Maehashi, K. Maruya, K. Domen, K. Aika and T. Onishi, *Chem. Lett.*, 747 (1984).
13. T. Yamaguchi, H. Sasaki, and K. Tanabe, *Chem. Lett.*, 1017 (1973).
14. B. H. Davis and P. Ganesan, *Ind. Eng. Chem. Prod. Res. Dev.*, **18**, 191 (1979).
15. T. Iizuka, Y. Tanaka, and K. Tanabe, *J. Catal.*, **76**, 1 (1982).
16. P. Turlier, J. A. Dalmon, and G. A. Martin, *Stud. Surf. Sci. Catal.*, **11**, 203 (1982).
17. R. Szymanski, H. Charcosset, P. Gallezot, J. Massardier, and L. Tournayan, *J. Catal.*, **97**, 366 (1986).
18. J. R. Sohn and H. J. Kim, *J. Catal.*, **101**, 428 (1986).
19. J. R. Sohn, H. W. Kim, and J. T. Kim, *J. Mol. Catal.*, **41**, 379 (1987).
20. J. R. Sohn and H. W. Kim, *J. Mol. Catal.*, **52**, 361 (1989).
21. J. R. Sohn and A. Ozaki, *J. Catal.*, **61**, 29 (1980).
22. M. J. Torralvo, M. A. Alario, and J. Soria, *J. Catal.*, **86**, 473 (1984).
23. A. Clearfield, *Inorg. Chem.*, **3**, 146 (1964).
24. J. R. Sohn and H. J. Jang, *J. Mol. Catal.*, **64**, 349 (1991).
25. A. Cimino, B. A. DeAngelis, A. Luchetti, and G. Minelli, *J. Catal.*, **45**, 316 (1976).
26. R. Merryfield, M. McDaniel, and G. Parks, *J. Catal.*, **77**, 348 (1982).
27. A. R. Gonzalez-Elipe, J. P. Espinos, A. Fernandez, and G. Munuera, *Appl. Surf. Sci.*, **45**, 103 (1990).
28. L. P. Hammett and A. J. Deyrup, *J. Am. Chem. Soc.*, **54**, 2721 (1932).
29. F. G. A. Olah, G. K. S. Prakash, and J. Sommer, *Science*, **206**, 13 (1979).
30. M. Itoh, H. Hattori and K. Tanabe, *J. Catal.*, **35**, 225 (1974).
31. V. A. Dzisko, Proc. 3rd Intn. Congr. Catalysis, Amsterdam, Vol. 1, No. 19 (1964).
32. M. Miura, Y. Kubota, T. Iwaki, K. Takimoto, and Y. Muraoka, *Bull. Chem. Soc. Jpn.*, **42**, 1476 (1969).
33. E. P. Parry, *J. Catal.*, **2**, 371 (1963).
34. M. C. Kung and H. H. Kung, *Catal. Rev-Sci. Eng.*, **2**, 425 (1985).
35. G. Connell and J. A. Dumesic, *J. Catal.*, **105**, 285 (1987).